

Title	Numerical visualization on melting and solidification of micron-sized metallic particles by laser irradiation
Author(s)	Takase, Kazuyuki; Muramatsu, Toshiharu; Shoubu, Takahisa
Citation	Transactions of JWRI. 39(2) P.1-P.3
Issue Date	2010-12
Text Version	publisher
URL	<a href="http://hdl.handle.net/11094/8423">http://hdl.handle.net/11094/8423</a>
DOI	
rights	
Note	

*Osaka University Knowledge Archive : OUKA*

<https://ir.library.osaka-u.ac.jp/>

Osaka University

# Numerical visualization on melting and solidification of micron-sized metallic particles by laser irradiation<sup>†</sup>

TAKASE Kazuyuki\*, MURAMATSU Toshiharu\*\*, SHOBU Takahisa\*\*\*

**KEY WORDS:** (Numerical simulation) (Laser welding) (Thermal-hydraulics) (Phase change) (Metallic particles) (Melting) (Solidification) (temperature) (liquid metal) (repair technology)

## 1. Introduction

Aiming at the enhancement of safety of currently operated nuclear reactors, development of a repair technology using laser welding [1] has been performed. An experimental study on welding of micron-sized metallic particles on a stainless steel plate by laser irradiation has already been carried out. Moreover, an analytical study was also begun to predict numerically the experimental results. The micron-sized metallic particle that is made of iron is heated by the laser irradiation and then melts and finally the solid metallic particle changes perfectly to the liquid metal. After a long time, the liquid metal solidified the solid metal with decreasing the temperature. This paper describes visualized numerical simulation results of the melting and solidification behavior of the micron-sized metallic particles that change from the solid to liquid and the liquid to solid.

## 2. Governing equations

Governing equations consist of gas and liquid phases as follows:

-Mass conservation;

$$\frac{\partial}{\partial t}(\alpha_g \rho_g) + \frac{\partial}{\partial x_j}(\alpha_g \rho_g U_{g,j}) = \Gamma \quad (1)$$

$$\frac{\partial}{\partial t}(\alpha_l \rho_l) + \frac{\partial}{\partial x_j}(\alpha_l \rho_l U_{l,j}) = -\Gamma \quad (2)$$

-Momentum conservation;

$$\begin{aligned} \frac{\partial U_{g,i}}{\partial t} + U_{g,j} \frac{\partial U_{g,i}}{\partial x_j} = & -\frac{1}{\rho_g} \frac{\partial P}{\partial x_i} - \frac{M_{g,i}^{int}}{\alpha_g \rho_g} \\ & - \frac{\Gamma^+}{\alpha_g \rho_g} (U_{g,i} - U_{l,i}) + \frac{1}{\alpha_g \rho_g} \frac{\partial \tau_{g,ij}}{\partial x_j} + g_i \end{aligned} \quad (3)$$

$$\begin{aligned} \frac{\partial U_{l,i}}{\partial t} + U_{l,j} \frac{\partial U_{l,i}}{\partial x_j} = & -\frac{1}{\rho_l} \frac{\partial P}{\partial x_i} - \frac{M_{l,i}^{int}}{\alpha_l \rho_l} \\ & - \frac{\Gamma^-}{\alpha_l \rho_l} (U_{g,i} - U_{l,i}) + \frac{1}{\alpha_l \rho_l} \frac{\partial \tau_{l,ij}}{\partial x_j} + g_i \end{aligned} \quad (4)$$

-Internal energy conservation;

$$-P \left[ \frac{\partial \alpha_g}{\partial t} + \frac{\partial (\alpha_g U_{g,j})}{\partial x_j} \right] + q_g^w + q_g^{int} + \Gamma \cdot h_g^{sat} \quad (5)$$

$$\begin{aligned} \frac{\partial}{\partial t}(\alpha_l \rho_l e_l) + \frac{\partial (\alpha_l \rho_l e_l U_{l,j})}{\partial x_j} = \\ -P \left[ \frac{\partial \alpha_l}{\partial t} + \frac{\partial (\alpha_l U_{l,j})}{\partial x_j} \right] + q_l^w + q_l^{int} - \Gamma \cdot h_l^{sat} \end{aligned} \quad (6)$$

## 3. Analytical conditions

Figure 1 shows the analytical geometry, which represents the experimental condition. 12x12 metallic particles are set into a slit on a metallic plate. Each of them is made of iron. The outer diameter of the metallic particle is 0.04 mm. The size of the slit is 0.48 mm square and 0.05 mm in depth. It briefly simulates any cracks on vessels or components of nuclear reactors. A laser beam is irradiated from the upper side into the slit. The shape of the laser beam is round as can be seen using red in Fig. 1, and the diameter is 0.48 mm.

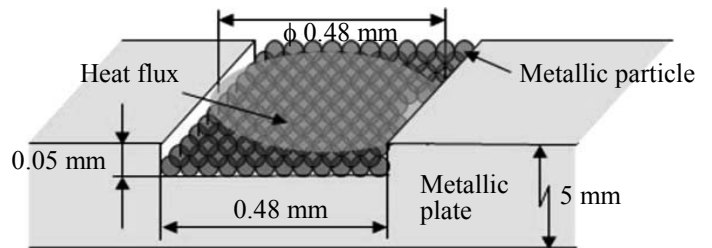


Fig. 1 Analytical geometry.

Figure 2 shows the phase change model from the solid to liquid phase and conversely the liquid to solid phase. The phase change behavior of the metallic particles with the laser irradiation is obtained from the liquid fraction,  $L_f$ , which is specified as the following equation:

<sup>†</sup> Received on 30 September 2010

\* Japan Atomic Energy Agency, Tokai, Ibaraki, Japan

\*\* Japan Atomic Energy Agency, Tsuruga, Fukui, Japan

\*\*\* Japan Atomic Energy Agency, Harima, Hyogo, Japan

$$L_f = \frac{T - T_s}{T_L - T_s} \quad (7)$$

Here,  $T$  represents the temperature of the metallic particle,  $T_s$  solidification temperature, and  $T_L$  melting temperature. The following three states related to  $T$  and  $L_f$  are considered:

- i) Solid state (at  $L_f=0$ ); when  $T < T_s$ ;
- ii) Liquid state (at  $L_f=1$ ); when  $T > T_L$ ; and,
- iii) Phase change state;  $T_s < T < T_L$ .

Therefore, change of enthalpy in the material from the solid to liquid by phase change is calculated from

$$h = h_0 + \int_{T_0}^T c_p dT + H_L L_f \quad (8)$$

Assumptions and conditions for the numerical analysis are as follows;

- 1) Constant heat flux given to the metal powders is 815 MW/m<sup>2</sup> and the heating time of the laser is 0.5 ms;
- 2) An ambient fluid around the metallic particles and plate is atmosphere;
- 3) Only metallic particles melt;
- 4)  $T_s=1809.9$  K and  $T_L=1810$  K are defined; and,
- 5) Two-phase flow simulation with the VOF method is used.

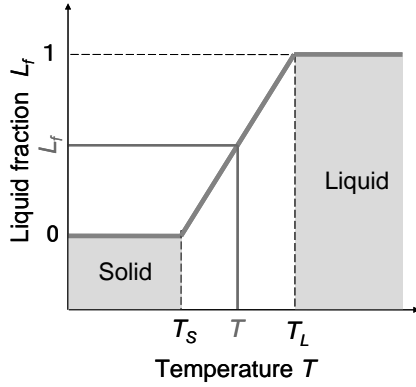


Fig. 2 Phase change model between solid and liquid phase.

#### 4. Results and discussion

Figure 3 shows predicted temperature distributions. The melting and solidification processes of the metallic particles due to the laser irradiation can be visualized numerically. Here, (a) is a result after 0.1 ms from the start of the calculation, and similarly, (b) is after 0.3 ms, (c) is 0.4 ms, and (d) is after 1 ms. The laser irradiation is completed at 0.5 ms. In Fig. 3, the blue means 500 K and the red means over 2200 K. First, the temperature of the metallic particle goes up in the heating region where the laser beam is irradiated as can be seen in Fig. 3(a). Next, the temperature of the metallic particle rises to the melting temperature (Fig. 3(b)) and the melting occurs as soon as it exceeds the melting temperature (Fig. 3(c)). With increasing the calculation time, almost all the metallic particles in the laser irradiation region melt and become liquid metal. Moreover, the metallic particles in a region where the laser is not irradiated are heated by thermal conduction, and melt. The laser irradiation is stopped after 0.5 ms. According to that, the heat moves from the high temperature region to the low temperature region due to the thermal conduction. As a result of this, the liquid metal region can be expanded. Then, by the thermal conduction to the metallic plate and the convection into the atmosphere, the temperature of the liquid metal decreases with time and the solidification takes place (Fig. 3(d)).

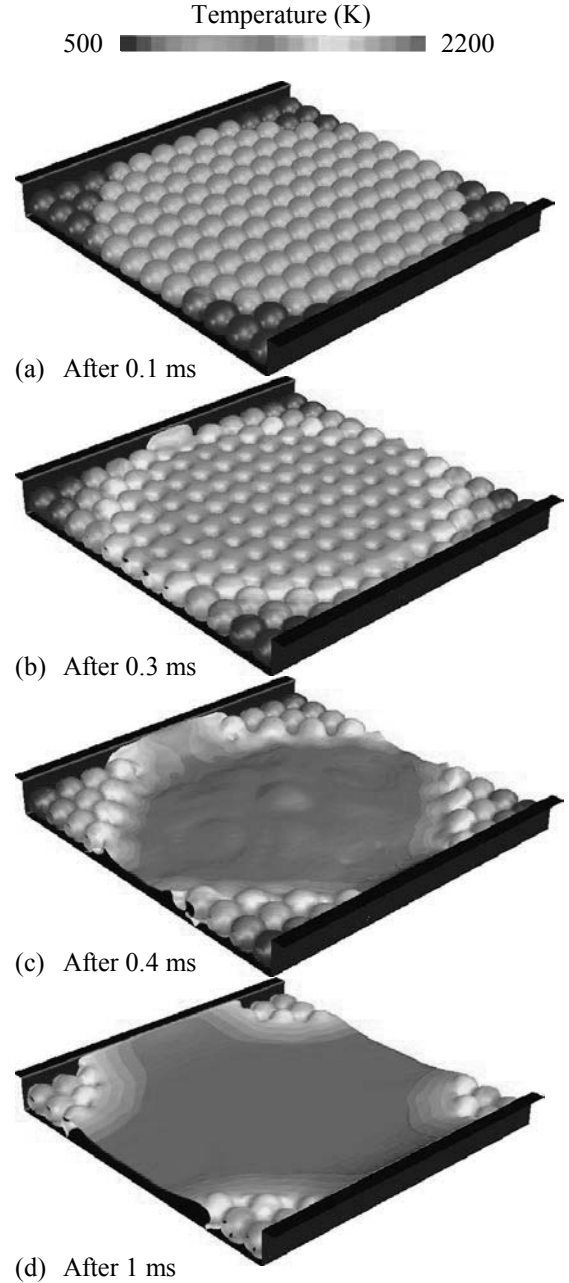


Fig. 3 Predicted temperature distributions at different time duration from the start of the calculation.

#### 5. Conclusions

A computational study on melting and solidification of micron-sized metallic particles was performed to clarify the possibility of the laser welding simulation. From the visualized results of the present study, we concluded that the welding simulation is possible and the present numerical approach will be effective.

#### 6. Nomenclature

- $e$  : Internal energy [J/kg]
- $g$  : Gravity [m/s<sup>2</sup>]
- $h^{sat}$  : Saturated enthalpy [J/kg]
- $M^{int}$  : Interfacial stress [kg/m<sup>2</sup>/s<sup>2</sup>]
- $P$  : Pressure [Pa]
- $q^{int}$  : Interfacial heat flux [W/m<sup>3</sup>]
- $q^w$  : Wall heat flux [W/m<sup>3</sup>]
- $t$  : Time [s]
- $U$  : Velocity [m/s]

$\alpha$  : Volume ratio

$\Gamma, \Gamma^+, \Gamma^-$  : Gas generation rate [ $\text{kg}/\text{m}^3/\text{s}$ ]

$\nu$  : Eddy viscosity [ $\text{m}^2/\text{s}$ ]

$\rho$  : Density [ $\text{kg}/\text{m}^3$ ]

$\tau$  : Shear stress tensor [ $\text{kg}/\text{m}/\text{s}^2$ ]

Subscripts

$g$  : Gas

$l$  : Liquid

$i, j$  : Spatial coordinate component

#### References

- [1] S. K. Maiti, et al.: Science&Technology of Welding and Joining, 8 (2003), pp.377-384.